Journal of Photochemistry and Photobiology A: Chemistry 226 (2011) 16–22

Contents lists available at SciVerse ScienceDirect

Journal of Photochemistry and Photobiology A: Chemistry

journal homepage: www.elsevier.com/locate/jphotochem

Photochemical production of formaldehyde, acetaldehyde and acetone from chromophoric dissolved organic matter in coastal waters

Warren J. de Bruyn, Catherine D. Clark*, Lauren Pagel, Chiyo Takehara

School of Earth and Environmental Sciences, Schmid College of Science and Technology, Chapman University, Orange, CA 92866, United States

ARTICLE INFO

Article history:
Received 9 February 2011
Received in revised form
20 September 2011
Accepted 3 October 2011
Available online 8 October 2011

Keywords:
Formaldehyde
Acetaldehyde
Acetone
Photochemistry
Coastal
California

ABSTRACT

Low molecular weight carbonyl compounds are produced photochemically from chromophoric dissolved organic matter (CDOM) in natural waters. Photoproduction rates for formaldehyde, acetaldehyde and acetone were measured in the laboratory using a pre-column 2,4-dinitrophenylhydrazine derivitization HPLC method as a function of optical properties (absorption coefficient, spectral slope) and irradiation time. Rates decreased linearly with decreasing absorption coefficient at 350 nm (a(350 nm)), a measure of CDOM levels, with substantial variability in low a(350 nm) beach waters. Apparent quantum yields (Θ) were unchanged for a(350 nm) = 2–16 m^{-1}, but increased rapidly (×5) for beach waters with low a(350 nm) values. Θ increased linearly with increasing spectral slope for beach waters, consistent with enhanced production efficiency with photobleaching of CDOM in coastal waters. Θ trends with oxygen and molecular reaction probes (hydroxyl radical scavengers and producers) suggested a combination of direct photolysis and singlet oxygen quenching as primary production mechanisms.

1. Introduction

Chromophoric dissolved organic matter (CDOM) refers to a spectrum of highly complex macromolecular colored materials that include humic substances [1]. Most CDOM in coastal waters comes from riverine or wetland inputs of terrestrially derived materials from plant degradation, but CDOM may also be produced from grazing phytoplankton and viral-induced lysis in the ocean [2,3]. When chromophoric dissolved organic matter (CDOM) absorbs light, it initiates a series of processes in natural waters which play a significant role in the global carbon cycle through remineralization of dissolved organic carbon (DOC) to carbon dioxide. Photochemical production of carbon dioxide from CDOM has been studied in coastal [4] and river waters [5], with multiple studies showing direct production of CO_2 from irradiated CDOM [6–9].

The complex photochemistry of CDOM [10] results in an indirect influence on CO_2 atmospheric and marine concentrations through the photochemical formation of LMW carbonyl compounds (e.g. acetone, acetaldehyde, formaldehyde, glyoxal, pyruvate) which are biologically available as an energy source for micro-organisms [11–13]. Photoproduction of LMW organic compounds has been shown to correlate with the concentration of UV-absorbing CDOM (as measured by initial absorbance and fluorescence levels) [14], with enhanced photoproduction and higher concentrations of LMW compounds reported in the sea surface microlayer where CDOM is enriched vs. underlying surface waters [15].

LMW compounds photochemically produced in surface ocean waters may also be important atmospherically through air–sea gas exchange acting as a source to the atmosphere [18,22]. Oxygenated hydrocarbons are ubiquitous in the atmosphere with levels ranging from pptv to low ppbv (e.g. 400–800 pptv for acetaldehyde and 800–1200 pptv for methanol) [16]. They react rapidly with OH [16], produce HO_x, O_3, CO, PAN and formaldehyde and contribute to particle formation in the atmosphere [17]. As a sink of OH and a source for HO_x and ozone, oxygenated hydrocarbons impact the atmospheric budgets of these oxidative species and over the last decade, attempts have been made to inventory sources and analyze atmospheric budgets of acetone, methanol, ethanol and acetaldehyde [17–21]. Although estimates have improved, significant discrepancies remain. In particular, the role of the oceans as a source or sink for oxygenated hydrocarbons is one of the largest sources of uncertainty in global models [17,20]. Budget estimates are limited by the very small database of ocean mixed layer measurements and a limited understanding of processes controlling levels in seawater [17,20].

In spite of their potential significance, there have been limited studies of the photochemical production rates of LMW compounds in ocean waters reported in the literature. These have been conducted in a limited spatial range, primarily in and around the southeastern coastal region of the United States, specifically the

* Corresponding author. Tel.: +1 714 628 7341; fax: +1 714 532 6048.
E-mail address: cclark@chapman.edu (C.D. Clark).

1010-6030/$ – see front matter © 2011 Elsevier B.V. All rights reserved.
doi:10.1016/j.jphotochem.2011.10.002

west coast of Florida [23], Florida Bay and the Gulf of Mexico [24], and Biscayne Bay and Everglades waters off Florida [14,15]. Other study sites include Caribbean waters near the Bahamas [15], the Sargasso Sea [14,15] and the Orinoco River off the coast of Brazil [14].

We report here production rates of three LMW oxygen-containing compounds (acetone, acetaldehyde, formaldehyde) measured in coastal waters on the west coast of the USA. These studies represent the first production rate measurements of LMW compounds in this global region (near-shore Pacific waters of the western USA). These are also the first studies of LMW production from salt-marsh derived CDOM, since brackish inputs from tidally flushed systems dominate these semi-arid coastal waters for most of the year [25]. We also report and discuss results from mechanistic studies utilizing a suite of molecular probes.

2. Materials and methods

2.1. Water samples

Samples were collected from 8 easily accessible beach sites covering a 15 km stretch of coastline and 4 adjacent wetlands and salt marshes as source water sites in Orange County, Southern California, from April 2008 to March 2009; site details are given in Table 1. The source water sites are brackish tidally flushed salt marsh systems that are hydrologically linked to the coastal beach waters sampled. In the dry season in Southern California, river mouths act as tidally flushed estuaries and salt marshes are the major source of CDOM to the surf zone [25]. The salt marshes sampled have been previously described [25,26]. Samples were collected from ankle-deep surf-zone waters on an incoming wave with a 1 m sampling scoop arm and vacuum filtered at the lab through glass fiber filters (GF/F; nominal pore size 0.7 μm; Whatman International Ltd). Samples were stored in the dark at 4 °C for production experiments.

2.2. HPLC analyses

Formaldehyde, acetaldehyde and acetone concentrations were quantified with a pre-column 2,4-dinitrophenylhydrazine (DNPH) derivitization HPLC method (Agilent 1100; Novapak C-18 (4 μm) column; UV detection at 370 nm; [15,24]). The DNPH (Aldrich) was re-crystallized twice from acetonitrile (ACN; Fisher; HPLC grade) and stored in the dark in air-tight Teflon vials prior to use. Twenty mg of re-crystallized DNPH was dissolved in 15 mL of a solution of concentrated hydrochloric acid (~12 M; Pharmco; ACS Reagent grade), water and ACN mixed in a 2:5:1 (v/v) ratio. Any carbonyl contamination in the resultant DNPH solution was removed by 2 successive extractions with carbon tetrachloride (Sigma–Aldrich Chromasolv for HPLC; 99.9%) just prior to use. To derivatize irradiated samples, 200 μL of DNPH solution was added to a 20 mL water sample in a 22 mL Teflon vial and the reaction allowed to proceed for 60 min before extraction and pre-concentration on C18 Sep-Pak cartridges (Supelco). Prior to use, cartridges were cleaned with 20 mL ACN and 10 mL of distilled water (DI; commercial Sparkletts Distilled). The derivatized sample was passed through the conditioned extraction cartridge at a flow rate of 10–15 mL min^{-1}. Excess reagent was washed off the cartridge with 25 mL of a 17% ACN (v/v) solution in DI followed by 5 mL of DI. Carbonyl hydrazones were eluted from the cartridge with 1 mL ACN into Teflon vials. Prior to HPLC analysis, extracts were reduced to dryness with a stream of carbonyl free nitrogen gas (Oxygen Services Co.; UHP) at room temperature and redissolved in 2 mL of a 10% ACN (v/v) solution in DI for a 10-fold enrichment. Two mL of the enriched sample was injected directly onto the Novapak C-18 column (Waters). To minimize potential contamination, extractions and derivitizations were carried out in a fume hood in a small solvent-free laboratory used only for this work. Carbonyl hydrazones were eluted using a two-solvent gradient: solvent A was 10% ACN (v/v) solution in DI adjusted to a pH of 2.6 with 10 N sulfuric acid (Sigma–Aldrich); solvent B was 100% ACN. The gradient was: isocratic at 35% B for 2 min; 35–53% B in 4 min; isocratic at 40% B for 8 min; 40–80% B in 10 min; and isocratic at 100% B for 15 min. Column flow rate was 1.5 mL min^{-1}; column temperature was controlled at 25 °C.

Table 1
GPS coordinates for wetland source and coastal beach sites sampled in Orange County, Southern California, USA.

Site	Type	Latitude	Longitude
Crystal Cove State Beach	Beach	33.574N	117.840W
Doheney State Beach	Beach	33.46198N	117.068285W
Talbert Marsh	Beach	33.634702N	117.960291W
Huntington Beach Pier	Beach	33.65392N	118.00065W
Laguna Beach Cliffs	Beach	33.543827N	117.798328W
Laguna Beach Pier	Beach	33.54211N	117.788458W
Newport Beach	Beach	33.607257N	117.93025W
Seal Beach	Beach	33.73883N	118.107491W
Quail Springs	Source	33.65808N	117.78123W
Red Hill	Source	33.72206N	117.82559W
Turtle Ridge	Source	33.63335N	117.82384W
Upper Newport Back Bay	Source	33.64846N	117.86687W

2.3. Irradiations

Filtered water samples were irradiated in the laboratory with a 300 W ozone-free Xenon lamp (Oriel Instruments; Model 6292) from 300 to 400 nm (band pass filter). Filtering removes effects due to biological activity and light scattering artifacts from particulate material, but does not affect the photochemistry of the CDOM [14]. Twenty-five mL water samples were irradiated for 60 min in 10-cm path length cylindrical quartz cells. Samples were agitated throughout the irradiation with a magnetic stirrer bar to ensure homogeneous mixing and light exposure. A 1 cm × 1 cm quartz cell with DI water was placed in front of the sample cell as an IR filter. A cooling fan (Radio Shack; placed at 90° to the side) cooled the sample cell. The temperature inside the sample cell measured by a thermocouple probe in trial runs increased by <1.5 °C within 5 min of irradiation, and remained constant throughout the remainder of the irradiation time. The photon flux was measured by chemical actinometry (nitrite/benzoic acid/hydroxybenzoic acid method [27,28]) to be 5.6×10^{19} photons m^{-2} s^{-1}. For comparison purposes, selected irradiations were later replicated with a recently acquired solar simulator (Luzchem SolSim) with a similar total flux of 3.7×10^{19} photons m^{-2} s^{-1} (as measured by actinometry) to assess the importance of wavelengths <300 nm for the solar simulator vs. the filtered Xenon lamp (band pass filter 300–400 nm). Quantum yields were higher in the solar simulator by factors of 1.2, 9 and 3 for formaldehyde, acetaldehyde and acetone respectively, suggesting that approximately 20% of the formaldehyde, 90% of the acetaldehyde and 70% of acetone would be produced at wavelengths <300 nm in the environment. These numbers were estimated by assuming that the increase in quantum yield was due to the wavelengths below 300 nm (for example, for acetaldehyde, an increase of a factor of 9 for the solar simulator vs. the lamp corresponds to a net contribution of 8/9 or 90% from the additional lower wavelengths). Quantum yields reported here have not been scaled to account for production at wavelengths <300 nm. To estimate real world values, quantum yields should be scaled based on the scaling factors above. All data shown in figures are from irradiation with the filtered Xenon lamp system. All oxygenated hydrocarbon yields were measured relative to an un-irradiated sample i.e. the un-irradiated sample was extracted and derivitized in parallel with the irradiated sample.

2.4. Optical properties

Absorbance spectra from 200 to 700 nm were obtained with a UV/VIS spectrophotometer (Agilent Technologies, Model 8453) using quartz cylindrical cells with a 10 cm path length. Absorbance was transformed to absorption coefficient (a, m^{-1}) by multiplying the measured absorbance at 350 nm by 2.303 and dividing by the path length in m [29]; 350 nm is one of the wavelengths commonly reported for CDOM absorbance [30,31]. Spectral slopes (S, nm^{-1}) for 300–400 nm region were calculated from Eq. (1):

$$-S = \frac{\ln \text{Abs}/A_0}{\lambda - \lambda_0} \quad (1)$$

where Abs is the absorbance (in m^{-1}) at wavelength λ and A_0 is the absorbance at a reference wavelength λ_0 [32–34].

2.5. Mechanistic probe experiments

Dimethyl sulfoxide (DMSO), an OH radical scavenger [35], was added to a Back Bay water sample to create solutions of 1–100 mmol L^{-1} DMSO and LMW compound production measured after a 60 min irradiation. Solutions containing 1–10 mmol L^{-1} nitrate, an OH radical producer [36,37], were produced by adding sodium nitrate ($NaNO_3$; Sigma) to a Back Bay sample and measuring net production after 60 min of irradiation. Oxygen effect experiments were also carried out by sparging a Back Bay water sample for 20 min prior to irradiation (flow rate = 100 mL min^{-1}) with ultra high-purity oxygen and air (Oxygen Services Co.). Quartz cells were sealed prior to irradiation. Accounting for any effects due to losses during purging was determined by comparison to the results for air at the same flow-rate.

3. Results

3.1. Absorption coefficients

Photochemical production rates and optical properties were measured for all 12 sites. Absorption coefficients can be used as a measure of how much CDOM is present in the water or how photo-active the CDOM is; this decreases as the CDOM is diluted or photochemically bleached on exposure to sunlight [30,38]. Absorption coefficients at 350 nm (a(350 nm)) ranged by a factor of 2.4 (8.7–20.6 m^{-1}) for the estuarine water samples and by a factor of 10 (0.27–2.7 m^{-1}) for the seawater samples. Absorption coefficients decreased from an average source water value of 16.1 ± 5.3 m^{-1} to an average seawater value of 0.98 ± 0.68 m^{-1}. Based on the observed range in a(350 nm), CDOM levels were at least an order of magnitude lower in the beach samples relative to the estuarine samples.

3.2. Photochemical production

In Fig. 1 we show concentrations of acetone, acetaldehyde and formaldehyde as a function of irradiation time. Acetone concentrations increased to 10 nmol L^{-1} over the course of a 3 h irradiation, whereas acetaldehyde increased to 120 nmol L^{-1} and formaldehyde reached 240 nmol L^{-1}. Acetone and acetaldehyde concentrations increased linearly over 3 h, but the increase was slightly non-linear for formaldehyde. Specifically, R^2 for a linear fit to the formaldehyde data is 0.989, whereas the fit to a second order polynomial has $R^2 = 0.998$. This decrease in observed rate at longer irradiation times may be due to the decreasing absorbance of CDOM in the sample as it is photobleached or to the depletion of oxygen [5].

Production rates are shown as a function of absorption coefficient for all samples in Fig. 2. Rates appear to increase linearly

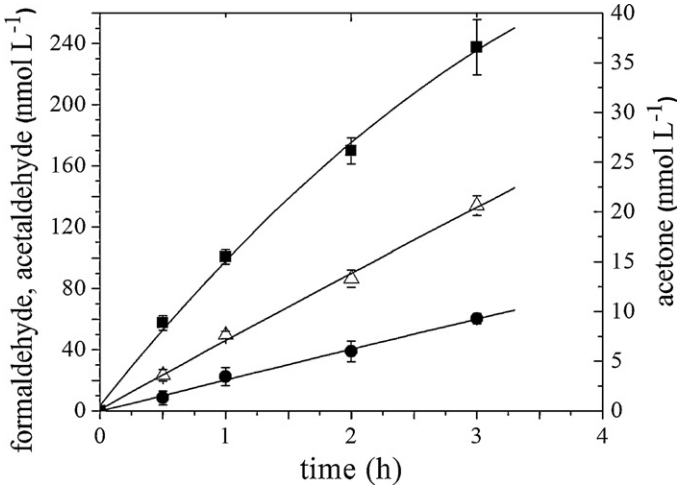

Fig. 1. Formaldehyde (■), acetaldehyde (△) and acetone (●) concentrations (in nmol L^{-1}) as a function of irradiation time (in h). Error bars are 1σ of the mean of three irradiations. R^2 for formaldehyde, acetaldehyde and acetone linear fits are 0.989, 0.998 and 0.996 respectively. The fit shown for formaldehyde is a second order polynomial ($R^2 = 0.998$).

with a(350 nm) consistent with the work of Kieber et al. [14]. However, care should be taken in interpreting Fig. 2 since the higher a(350 nm) estuarine waters are causing the plot to appear linear; if just the seawater samples are considered, the correlation is not as strong. For example, r^2 decreases from 0.985 to 0.216 for formaldehyde, 0.886 to 0.694 for acetaldehyde and 0.372 to 0.16 for acetone. We attribute the lower correlation coefficients for acetone either to natural variability between sites or the lower concentrations for acetone being closer to the measurement detection limits. A more meaningful comparison would be to normalize photoproduction to the CDOM content of the sample i.e. calculate quantum yields.

3.3. Apparent quantum yields

Quantum yields, a measure of photoproduction efficiency, for these photochemical processes would ideally be given by dividing the number of molecules of product produced by the number of photons absorbed by the chromophore. A quantum yield of 1 would mean that every photon absorbed produces a photoproduct molecule. However, since the LMW products are likely to be

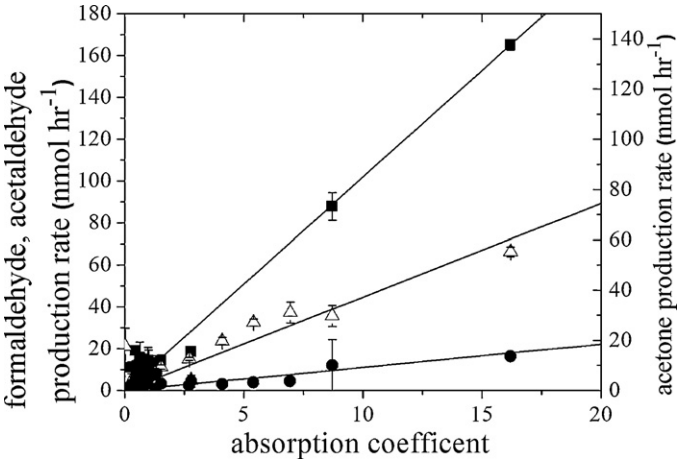

Fig. 2. Formaldehyde, acetaldehyde and acetone production rates (in nmol L^{-1} h^{-1}) as a function of a(350 nm) (in m^{-1}). Error bars are 1σ of the mean of three irradiations. R^2 for formaldehyde, acetaldehyde and acetone are 0.985, 0.886 and 0.372 respectively.

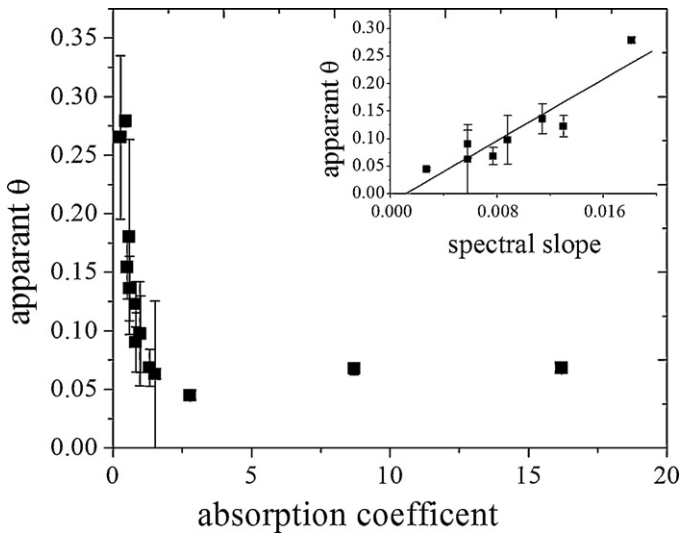

Fig. 3. Apparent quantum yield (Θ) for formaldehyde vs. absorption coefficient at 350 nm (in m^{-1}). Inset figure shows a plot of Θ vs. spectral slope (in nm^{-1}). Line shown is from a linear regression ($r^2 = 0.857$). Error bars are 1σ ($n = 3$).

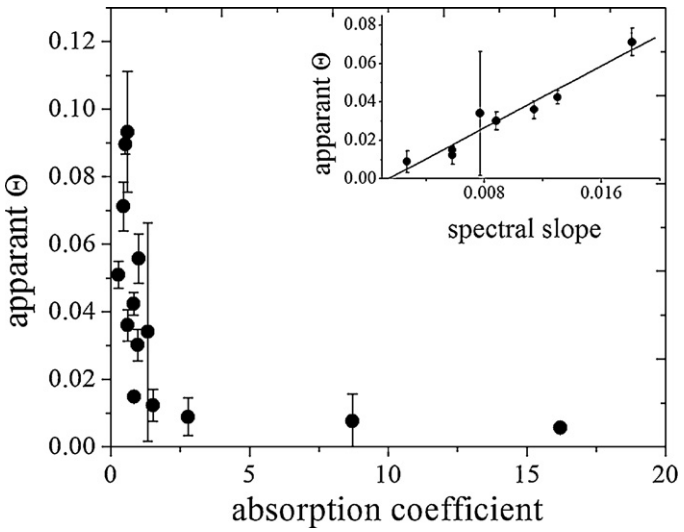

Fig. 5. Apparent quantum yield (Θ) for acetone vs. absorption coefficient at 350 nm (in m^{-1}). Inset figure shows a plot of Θ vs. spectral slope (in nm^{-1}). Line shown is from a linear regression ($r^2 = 0.973$). Error bars are 1σ ($n = 3$).

produced via secondary reactions and CDOM is not well characterized, a true quantum yield cannot be calculated. Instead, apparent quantum yields (Θ) were estimated by the method of Moore et al. [39], where the production rate is normalized to a(350 nm) and the measured lamp photon flux. While not a true quantum yield, this allows for comparison between samples with different a(350 nm).

In Figs. 3–5 we show the apparent quantum yields (Θ) for the three compounds as a function of a(350 nm). We would expect Θ to be independent of a(350 nm) if the photoproduction efficiency remains the same for different CDOM-containing waters. However, we observed a significant increase in Θ for the low a(350 nm) beach samples (source waters: 0.045–0.068 formaldehyde, 0.0101–0.0274 acetaldehyde, 0.0001–0.008 acetone vs. seawater: 0.045–0.279 formaldehyde, 0.034–0.122 acetaldehyde, 0.009–0.093 acetone). Average source water Θ's were 0.0578 ± 0.0019, 0.0198 ± 0.0016 and 0.0048 ± 0.0042 for formaldehyde, acetaldehyde and acetone respectively. Corresponding average seawater Θ's were 2–10 times higher (0.132 ± 0.024, 0.062 ± 0.006, 0.045 ± 0.009 respectively). We obtained similar results using a wavelength of 300 nm to calculate Θ, another common wavelength reported for CDOM [31].

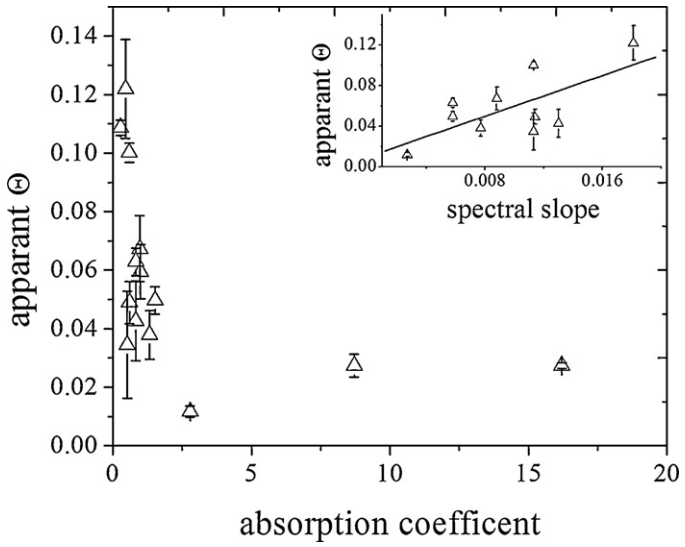

Fig. 4. Apparent quantum yield (Θ) for acetaldehyde vs. absorption coefficient at 350 nm (in m^{-1}). Inset figure shows a plot of Θ vs. spectral slope (in nm^{-1}). Line shown is from a linear regression ($r^2 = 0.461$). Error bars are 1σ ($n = 3$).

3.4. Spectral slope dependence

To further examine why Θ for the low absorbing beach waters varies so significantly, we calculated spectral slopes for these samples. Seawater spectral slopes ranged from 0.006 to 0.018 with an average of $0.010 \pm 0.004\ nm^{-1}$, within the range of s values previously measured in this coastal region [25,40]. Insets in Figs. 3–5 show that Θ for the seawater samples increases linearly with increasing spectral slope for all 3 compounds. Changes in s are due to the loss or formation of higher molecular weight aromatic material [30,41,42]. Generally, increasing s values from high-absorbing coastal to lower-absorbing oceanic off-shore waters have been attributed to photodegradation of the terrestrial end-member [30,34,43,44] or conservative mixing of a high s oceanic end-member with a low s terrestrial end-member [45]. The observed correlation of Θ with s suggests a relationship between the efficiency of LMW production and the structural characteristics of CDOM, which can be altered through photo- or microbial degradation processes as terrestrial material is exported into coastal waters i.e. a water body can have the same absorption coefficient as another but demonstrate much higher production of these compounds if it has a higher spectral slope value.

3.5. Mechanistic studies

To evaluate possible mechanisms, we carried out steady-state photochemical experiments using molecular probes. In Fig. 6, we show Θ as a function of nitrate concentration. Direct photolysis of nitrate ions produces OH radicals in natural waters via an O^- intermediate [36,37]. Although nitrate occurs naturally in natural waters at micromolar concentrations, we added elevated millimolar concentrations as a probe to see if production increased with higher nitrate concentrations. Θ for all 3 compounds doubled as nitrate concentration increased from 1 to $7 \times 10^{-3}\ mol\ L^{-1}$, suggesting an OH intermediate contributes to the photoproduction of all three oxygenated hydrocarbons. In Fig. 7, Θ is shown as a function of added DMSO, an OH radical scavenger [35], for acetaldehyde and acetone. This was not a meaningful test for formaldehyde because

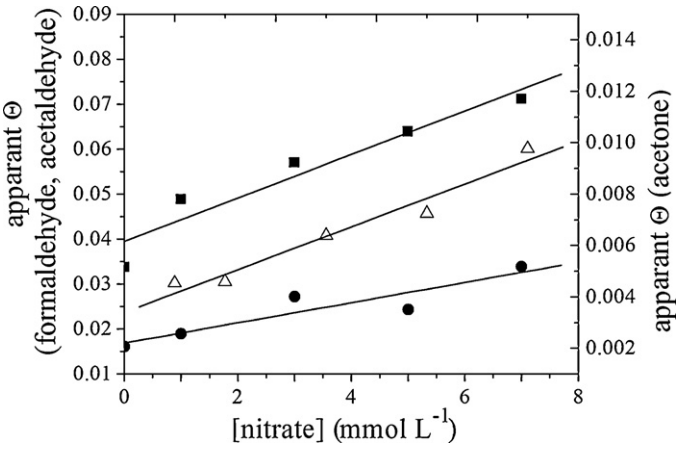

Fig. 6. Apparent quantum yields (Θ) for formaldehyde (■), acetaldehyde (△) and acetone (●) as a function of nitrate concentration (in mmol L^{-1}). Lines shown are from linear regressions.

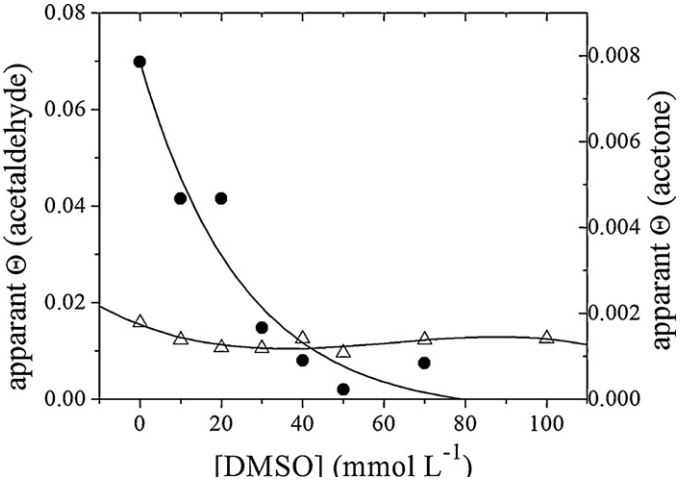

Fig. 7. Apparent quantum yields (Θ) for acetaldehyde (△) and acetone (●) as a function of DMSO concentration (in mmol L^{-1}). Lines shown for ease of viewing.

DMSO and OH react to produce formaldehyde [46]. For acetaldehyde and acetone, Θ decreased as the DMSO concentration was increased. Acetone yields decreased by 90% at 50×10^{-3} mol L^{-1} DMSO, suggesting an OH radical driven process is the dominant production mechanism. Acetaldehyde yields decreased by 30% at 20×10^{-3} mol L^{-1} DMSO and then remained relatively constant, suggesting an OH radical driven process contributes to, but is not the dominant mechanism for, acetaldehyde production in natural waters.

The production of formaldehyde, acetaldehyde and acetone were compared for air vs. oxygen-sparged solutions to test the mechanistic importance of oxygen (per [14]). In a previous study of CO_2 production, Xie et al. [5] observed enhanced photooxidation rates of DOM in river waters with increasing oxygen content, where the photodecarboxylation process was expressed as $RCOOH + \frac{1}{2}O_2 \rightarrow ROH + CO_2$. Our results are given in Table 2.

Table 2
Concentrations (in nmol L^{-1}) of formaldehyde, acetaldehyde and acetone produced after irradiation of air- and oxygen-saturated Back Bay water samples for 1 h.

	Air	Oxygen
Formaldehyde	89 ± 2	112 ± 2
Acetaldehyde	45 ± 2	47 ± 4
Acetone	7.1 ± 0.3	12 ± 1

Sparging with pure oxygen gas increased formaldehyde production by 25% and acetone by 70% relative to sparging with air. The change in acetaldehyde production was not significant.

4. Discussion

4.1. Apparent quantum yields

For the source waters, photoproduction efficiency (Θ) had a maximum of 1% for acetone, 7% for formaldehyde and 3% for acetaldehyde. Maximum values were higher in seawater, but followed the same trend with formaldehyde being the highest: 9% acetone, 30% formaldehyde and 12% acetaldehyde. Formaldehyde and acetaldehyde showed similar increases of a factor of 4 from source to seawaters, while acetone's Θ increased by a factor of 10. We attribute increases in Θ from the source to seawaters to increased photodegradation resulting in more aged materials that are easier to break down into smaller LMW compounds i.e. at least on these timescales, photodegradation of CDOM produces partially degraded material that is initially more susceptible to further degradation. Irradiation of CDOM in riverine to marine transition zones has been shown to result in changes like a decrease in size distribution, increased bioavailability, production of dissolved inorganic carbon compounds and a loss of chromophores (photobleaching of optical absorbance) and structural components like lignin phenolic compounds [9 and references therein].

4.2. Production pathways

CDOM has a complex photochemistry, where initial absorption of light produces an excited triplet state (Eq. (2)) which can produce reactive transients and photoproducts by a range of pathways [47]. The primary initial pathways are direct photolysis from the triplet excited state of CDOM (Eq. (3), produces smaller organic compounds), photoionization (Eq. (4), produces a CDOM cation and hydrated electron) and quenching of the triplet excited state of CDOM by ground-state oxygen (Eq. (5), generates superoxide which reacts with water (Eq. (6)) to produce reactive peroxide and radical species).

$$\text{Lightabsorption} \quad \text{CDOM} + h\nu \rightarrow {}^3\text{CDOM}^* \tag{2}$$

$$\text{Direct photolysis} \quad {}^3\text{CDOM}^* \rightarrow \text{products} \tag{3}$$

$$\text{Photoionization} \quad {}^3\text{CDOM}^* \rightarrow \text{CDOM}^+ + e_{aq}{}^- \tag{4}$$

$$\text{Quenching} \quad {}^3\text{CDOM}^* + O_2 \rightarrow \text{CDOM}^+ + O_2{}^- \tag{5}$$

$$\text{Radical production} \quad O_2{}^- + H_2O \rightarrow OH^- + HO_2^\bullet \rightarrow H_2O_2, OH^\bullet \text{etc.} \tag{6}$$

Many of the products and subsequent chemistry of Eqs. (5) and (6) have been studied in seawater [48], specifically the reaction of oxygen molecules with photo-excited CDOM to generate superoxide $O_2{}^-$ and its conjugate acid $HO_2^\bullet$ which dismutates to form H_2O_2 [49]. Subsequent secondary reactions of H_2O_2 generate hydroxyl radicals in natural waters [48]. Photochemical reactions from the low micromolar levels of nitrate and nitrite ions found in seawater also produce hydroxyl radicals [36,37]. If hydroxyl radicals play a significant role in LMW production, the addition of an OH radical scavenger might be expected to decrease production whereas the addition of an OH radical producer should increase production. In addition, if the quenching of the triplet excited-state of CDOM by oxygen to produce superoxide (Eq. (5)) plays a major role in the

production of the LMW compounds measured here through secondary reaction products, the addition of oxygen should increase LMW production. However, since oxygen can also directly quench the triplet state to produce ground-state CDOM and singlet oxygen $^1O_2$ [10], additional oxygen would cause a decrease in production if direct photolysis (Eq. (3)) is the pathway dominating the production mechanism. Which effect dominates will depend on the degree of competition between these 2 pathways with oxygen i.e. on the relative quantum yields or efficiencies of these 2 reactions relative to each other.

Based on the mechanistic probe and oxygen results described in section 3.5, it appears that formaldehyde and acetone have some similarities in production mechanism whereas acetaldehyde behaves differently. Specifically: (1) oxygen increased formaldehyde and acetone production but did not affect acetaldehyde; (2) Θ for all 3 compounds increased by a factor of 2 when nitrate, an OH radical producer was added; and (3) Θ decreased for acetaldehyde and acetone with the addition of DMSO, an OH radical scavenger; however, acetone yields decreased by 90% and acetaldehyde by 30%. Based on these results, it appears that formaldehyde and acetone production may proceed predominantly via an OH/O_2 pathway (Eqs. (5) and (6)) whereas another significant pathway for acetaldehyde may be direct photolysis (Eq. (3)) (or an hydrated electron intermediate (Eq. (5))), with some contribution from the OH/O_2 pathway. A potential explanation for no observed oxygen effect for acetaldehyde may be the competing inverse trends if both pathways contribute since oxygen increases production via Eq. (5) (quenching by oxygen to produce superoxide) but also decreases production via Eq. (3) (quenching of ^{3}CDOM* reducing direct photolysis products), i.e. the oxygen effects offset each other.

For acetaldehyde, our results are consistent with the work of Kieber et al. [14] but not for formaldehyde and acetone, since they reported no oxygen effect on the photoproduction of acetone, acetaldehyde and formaldehyde. Based on their measured action spectra and no oxygen impact, they concluded that these species were all likely produced by direct photolysis. However, it is important to note that the irradiation systems used in these two studies are different. Kieber et al. [14] used a 450-W medium pressure mercury vapor lamp system with wavelengths >290 nm which included more energetic UV; the UVB (280–320 nm) region of the solar spectrum was most efficient at producing LMW carbonyl compounds. By contrast, the lamp configuration in our study cuts off at 300 nm, excluding the more energetic (280–300 nm) portion of the UVB region and thus reducing the contribution of a direct photolysis mechanism.

Based on a comparison of the increased production rates for our solar simulator and filtered lamp system which have comparable total photon fluxes but some UV contribution below 300 nm for the solar simulator, approximately 20% of formaldehyde, 90% of acetaldehyde and 70% of acetone production would be due to wavelengths <300 nm in the environment. This is consistent with acetaldehyde production having a larger contribution from direct photolysis which would be more efficient at lower more energetic wavelengths, whereas an OH mechanism contributes to formaldehyde and acetone. The weaker positive trend observed for acetaldehyde for Θ vs. spectral slope (Fig. 4) vs. the strong correlation for formaldehyde and acetone (Figs. 3 and 5) might be due to direct photolysis contributing significantly to acetaldehyde production but not to formaldehyde and acetone. If this is the case, then as spectral slopes increase, photoproduction efficiencies increase largely through the OH pathway (which dominates acetone and formaldehyde production) rather than through increased direct photolysis, resulting in the stronger observed correlation for these two LMW carbonyls between Θ vs. spectral slope (correlation coefficients of 0.8 and 0.9 for formaldehyde and acetone vs. 0.4 for acetaldehyde). Since s increases when DOM undergoes photolysis and the proportion of higher molecular weight material (with more intense absorbance at red-shifted wavelengths) decreases [see for example 41], increasing production efficiencies appear to be associated with an increase in the proportion of low MW material in CDOM i.e. the more photodegraded the DOM, the more efficient the production of LMW carbonyls.

5. Conclusion

Previous production studies for these compounds on coastal waters dominated by large fresh water riverine inputs of terrestrial DOM [14,15,23,24] suggested that production varied linearly with absorption coefficient i.e. with CDOM levels and therefore that production efficiency was independent of absorbance and relatively constant in the environment. This has lead to the use of single quantum yields in global models [17]. In contrast production efficiencies measured in coastal waters dominated by salt marshes in this study increased significantly with increasing spectral slope, suggesting that the production efficiency of these LMW carbonyls may vary significantly regionally depending on CDOM source, aging and/or local loss processes. This has global significance because salt marshes are found in intertidal zones in the middle and high latitudes throughout the world and wetlands are among the most productive ecosystems based on net global primary productivity of carbon ($1300\,g\,C\,m^{-2}\,year^{-1}$) [50–52], Thus, these sites are potentially a significant source of LMW compounds from CDOM photolysis that may currently be underestimated by as much as a factor of 5–10 in global models based on previously published quantum yields for coastal waters dominated by riverine CDOM. Mechanistic studies were consistent with the photochemical production of acetaldehyde proceeding primarily via a direct photolysis pathway, whereas acetone and formaldehyde production is primarily via an OH/O_2 pathway.

Acknowledgements

This work was funded by Chapman University Faculty Development Grants and the National Science Foundation (OCE Grant #072528433). The authors thank undergraduate students Katie Ottelee, Charlie Hirsch and Benjamin Brahm for assistance with sampling, optical and actinometry measurements.

References

[1] E.M. Perdue, in: Hessen, Tranvik (Eds.), Ecological Studies: Aquatic Humic Substances, vol. 133, Springer-Verlag, Heidelberg, 1998, pp. 41–61 (Chapter 2).
[2] D.M. McKnight, G.R. Aiken, in: Hessen, Tranvik (Eds.), Ecological Studies: Aquatic Humic Substances, vol. 133, Springer-Verlag, Heidelberg, 1998, pp. 9–39 (Chapter 1).
[3] R.H. Benner, in: Hessen, Tranvik (Eds.), Ecological Studies: Aquatic Humic Substances, vol. 133, Springer-Verlag, Heidelberg, 1998, pp. 317–331 (Chapter 12).
[4] C.D. Clark, W.T. Hiscock, F.J. Millero, G. Hitchcock, L. Brand, R. Del, N. Vecchio, W. Blough, L. Miller, R.F. Ziolkowski, R.G. Chen, Zika, CDOM Distribution and carbon dioxide production on the Southwest Florida Shelf, Mar. Chem. 89 (2004) 145.
[5] H. Xie, O.C. Zafiriou, W.-J. Cai, R.G. Zepp, Y. Wang, Photooxidation and its effects on the carboxyl content of dissolved organic matter in two coastal rivers in the southeastern United States, Environ. Sci. Technol. 38 (2004) 4113–4119.
[6] W.L. Miller, R.G. Zepp, Photochemical production of dissolved inorganic carbon from terrestrial organic matter: significance to the oceanic organic carbon cycle, Geophys. Res. Lett. 24 (1995) 417–420.
[7] E. Granelli, P. Carlsson, C. Legrand, The role of C, N and P in dissolved and particulate organic matter as a nutrient source for phytoplankton growth, including toxic species, Aquat. Ecol. 33 (1999) 17–27.
[8] W.L. Miller, M.A. Moran, Interaction of photochemical and microbial processes in the degradation of refractory dissolved organic matter from a coastal marine environment, Limnol. Oceanogr. 42 (1997) 1317–1324.
[9] K. Mopper, D.J. Kieber, Photochemistry and the cycling of carbon, sulfur, nitrogen and phosphorus, Ch 9, in: Biogeochemistry of Marine Dissolved Organic Matter, Elsevier, 2002, p. 455.
[10] R.G. Zepp, Environmental photoprocesses involving natural organic matter, in: F.H. Frimmel, R.F. Christman (Eds.), Humic Substances and Their Role in the Environment, Wiley-Interscience, New York, 1988, pp. 193–214.

[11] M.A. Moran, R.G. Zepp, Role of photoreactions in the formation of biologically labile carbon from dissolved organic matter, Limnol. Oceanogr. 42 (1997) 1307.
[12] N. Bano, M.A. Moran, R.E. Hodson, Photochemical formation of labile organic matter from two components of dissolved organic carbon in a freshwater wetland, Aquat. Microb. Ecol. 16 (1998) 95–102.
[13] R.G. Zepp, T.V. Callaghan, D.J. Erikson, Effects of enhanced solar ultraviolet radiation on biogeochemical cycles, J. Photochem. Photobiol. 46 (1998) 69–82.
[14] R.J. Kieber, X. Zhou, K. Mopper, Formation of carbonyl compounds from UV-induced photodegradation of humic substances in natural waters: fate of riverine carbon in the sea, Limnol. Oceanogr. 35 (1990) 1503–1515.
[15] X. Zhou, K. Mopper, Photochemical production of low-molecular-weight carbonyl compounds in seawater and surface microlayer and their air–sea exchange, Mar. Chem. 56 (1997) 201–213.
[16] H.B. Singh, L.J. Slas, R.B. Chatfield, E. Czech, A. Fried, J. Walega, M.J. Evans, B.D. Field, D.J. Jacob, D. Blake, B. Heikes, R. Talbot, G. Sachse, J.H. Crawford, M.A. Avery, S. Sandholm, H. Fuelberg, Analysis of atmospheric distribution, sources and sinks of oxygenated volatile organic chemicals based on measurements over the Pacific during TRACE-P, J. Geophys. Res. 109 (2004) D15S07, doi:10.1029/2003JD003883.
[17] D.B. Millet, A. Guenther, D.A. Siegel, N.B. Nelson, H.B. Singh, J.A. de Gouw, C. warneke, J. Williams, G. Erdekens, V. Sinha, T. Karl, F. Flocke, E. Apel, D.D. Riemer, P.I. Palmer, M. Barkley, Global atmospheric budget of acetaldehyde: 3-D model analysis and constraints from in situ and satellite observations, Atmos. Chem. Phys. 10 (2010) 3405–3425.
[18] H. Singh, Y. Chen, A. Staudt, D. Jacob, D. Blake, B. Heikes, J. Snow, Evidence from the Pacific troposphere for large global sources of oxygenated organic compounds, Nature 410 (2001) 1078–1081.
[19] D.J. Jacob, B.D. Field, E.M. Jin, I. Bey, Q. Li, J.A. Logan, R.M. Yantosca, Atmospheric budget of acetone, J. Geophys. Res. 107 (D10) (2002) 4100, doi:10.1029/2001JD000694.
[20] D.B. Millet, D.J. Jacob, T.G. Custer, J.A. de Gouw, A.H. Goldstein, T. Karl, H.B. Singh, B.C. Sive, R.W. Talbot, C. Warneke, J. Williams, New constraints on terrestrial and oceanic sources of atmospheric methanol, Atmos. Chem. Phys. 8 (2008) 6887–6905.
[21] V. Naik, A.M. Fiore, L.W. Horowitz, H.B. Singh, C. Wiedinmyer, A. Guenther, J.A. de Gouw, D.B. Millet, P.D. Goldan, W.C. Kuster, A. Goldstein, Observational constraints on the global atmospheric budget of ethanol, Atmos. Chem. Phys. Dis. 10 (2010) 925–945.
[22] S.R. Arnold, M.P. Chipperfield, M.A. Blitz, D.E. Heard, M.J. Pilling, Photodissociation of acetone: atmospheric implications of temperature-dependent quantum yields, Geophys. Res. Lett. 31 (2004) LO7110, doi:10.1029/2003GLO19099.
[23] K. Mopper, W.L. Stahovec, Sources and sinks of low molecular weight organic carbonyl compounds in seawater, Mar. Chem. 19 (1986) 305–321, doi:10.1016/0304-4203(86)90052-6.
[24] D.J. Kieber, K. Mopper, Photochemical formation of glyoxylic and pyruvic acids in seawater, Mar. Chem. 21 (1987) 135–149.
[25] C.D. Clark, L.P. Litz, S.B. Grant, Saltmarshes as a source of chromophoric dissolved organic matter to Southern California coastal waters, Limnol. Oceanogr. 53 (2008) 1923.
[26] A.M. Pednekar, S.B. Grant, Y. Jeong, Y. Poon, C. Oancea, Influence of climate change, tidal mixing, and watershed urbanization on historical water quality in Newport Bay, a Saltwater Wetland and Tidal Embayment in Southern California, Environ. Sci. Technol. 39 (2005) 9071–9082.
[27] J.J. Jankowski, D.J. Kieber, K. Mopper, Nitrate and nitrite ultraviolet actinometers, Photochem. Photobiol. 70 (1999) 319–328.
[28] J.J. Jankowski, D.J. Kieber, K. Mopper, P.J. Neale, Development and intercalibration of ultraviolet solar actinometers, Photochem. Photobiol. 71 (2000) 431–440, doi:10.1562/0031-8655.
[29] C. Hu, F.E. Muller-Karger, R.G. Zepp, Absorbance, $a(300)$ and apparent quantum yield: a comment on common ambiguity in the use of these optical concepts, Limnol. Oceanogr. 47 (2002) 1261–1267.
[30] M.A. Moran, W.M. Sheldon Jr., R.G. Zepp, Carbon loss and optical property changes during long-term photochemical and biological degradation of estuarine dissolved organic matter, Limnol. Oceanogr. 45 (2000) 1254–1264.
[31] P. Kowalczuk, W.J. Cooper, M.J. Durako, A.E. Kahn, M. Gonsior, H. Young, Characterization of dissolved organic matter fluorescence in South Atlantic Bight with use of PARAFAC model: relationships between fluorescence and its components, absorption coefficients and organic carbon concentrations, Mar. Chem. 118 (2010) 22–36, 118.
[32] S.A. Green, N.V. Blough, Optical absorbance and fluorescence properties of chromophoric dissolved organic matter in natural waters, Limnol. Oceanogr. 39 (1994) 1903–1916.
[33] A. Seritti, D. Russo, L. Nannicini, R. Del Vecchio, DOC, absorbance and fluorescence properties of estuarine and coastal waters of the Morthern Tyrrhenian Sea, Chem. Spec. Bioavail. 10 (1998) 95–106.
[34] R.F. Whitehead, S. De Moro, S. Demers, M. Gosselin, P. Monfort, B. Mostajir, Interactions of ultraviolet B radiation, mixing and biological activity on photobleaching of natural chromophoric dissolved organic matter: a mesocosm study, Limnol. Oceanogr. 45 (2000) 278–291.
[35] P.P. Vaughan, N.V. Blough, Photochemical formation of hydroxyl radical by constituents of natural waters, Environ. Sci. Technol. 32 (1998) 2947–2953, doi:10.1021/es9710417.
[36] O.C. Zafiriou, M.B. True, Nitrite photolysis as a source of free radicals in productive surface waters, Geophys. Res. Lett. 6 (1979) 81–84.
[37] R.G. Zepp, J. Hoigne, H. Bader, Nitrate induced photo-oxidation of trace organic chemicals in water, Environ. Sci. Technol. 21 (1987) 443–450.
[38] C.L. Gallegos, T.E. Jordan, A.H. Hines, D.E. Weller, Temporal variability of optical properties in a shallow, eutrophic estuary: seasonal and interannual variability, Estuar. Coast. Shelf Sci. 64 (2005) 156–170, doi:10.1016/j.ecss.2005.01.013.
[39] C.A. Moore, C.T. Farmer, R.G. Zika, Influence of the Orininoco River on the hydrogen peroxide distribution and production in the Eastern Caribbean, J. Geophys. Res. 98 (1993) 2289–2298.
[40] C.D. Clark, W. De Bruyn, C.M. Hirsch, S.B. Jakubowski, Hydrogen peroxide measurements in recreational marine bathing waters in Southern California, USA, Water Res. 44 (2010) 2203–2210.
[41] J.R. Helms, A. Stubbins, J.D. Ritchie, E.C. Minor, D.J. Kieber, K. Mopper, Absorption spectral slopes and slope ratios as indicators of molecular weight, source and photobleaching, Limnol. Oceanogr. 53 (2008) 955–969.
[42] R. Del Vecchio, N.V. Blough, On the origin of the optical properties of humic substances, Environ. Sci. Technol. 38 (2004) 3885–3891, doi:10.1021/es049912h.
[43] M.S. Twardowski, P.L. Donaghay, Photobleaching of aquatic dissolved materials: absorption removal, spectral alteration and their relationship, J. Geophys. Res. 107 (2002), doi:10.1029/1999JC000281.
[44] C.A. Stedmon, S. Markager, H. Kaas, The optics of chromophoric dissolved organic matter (CDOM) in the Greenland Sea: an algorithm for differentiation between marine and terrestrially derived organic matter, Limnol. Oceanogr. 46 (2001) 2087–2093.
[45] C.A. Stedmon, S. Markager, Behavior of the optical properties of colored dissolved organic matter under conservative mixing, Estuar. Coast. Shelf Sci. 57 (2003) 973–979, doi:10.1016/S0272-7714(03)00003-9.
[46] Y. Lee, C. Lee, J. Yoon, Kinetics and mechanism of DMSO degradation by UV/H_2O_2 process, Water Res. 38 (2004) 2579–2588.
[47] J. Hoigne, B.C. Fau, W.R. Haag, F.E. Scully, R.G. Zepp, Aquatic humic substances as sources and sinks of photochemically produced transient reactants, Ch 23, in: Aquatic Humic Substances, Advances in Chemistry, vol. 23, American Chemical Society Publications, Washington, DC, 1988, pp. 363–381.
[48] W.J. Cooper, C. Shao, D.R.S. Lean, A.S. Gordon, F.E. Scully Jr., Factors affecting the distribution of H_2O_2 in surface waters, in: L.A. Baker (Ed.), Environmental Chemistry of Lakes and Reservoirs, Advances in Chemistry Series, vol. 237, American Chemical Society, Washington, DC, 1994, pp. 391–422.
[49] D.E. Cabelli, The reactions of HO_2/O_2^- radicals in aqueous solution, in: Z.B. Alfassi (Ed.), Peroxyl Radicals, John Wiley and Sons Ltd., New York, 1997, pp. 407–437.
[50] D.S. McLusky, M. Elliott, The Estuarine Ecosystem: Ecology, Threats and Management, 3rd ed., Oxford University Press, 2004.
[51] W.J. Mitsch, J.G. Gosselink, Wetlands, 3rd ed., Wiley, 2000.
[52] M. Tzortziou, C.L. Osburn, P.J. Neale, Photobleaching of dissolved organic material from a tidal marsh-estuarine system of the Chesapeake Bay, Photochem. Photobiol. 83 (2007) 782–792, doi:10.1562/2006-09-28-RA-1048.